OPEN

ORIGINAL ARTICLE

Topoisomerase IIα mediates TCF-dependent epithelial–mesenchymal transition in colon cancer

Q Zhou[1], AD Abraham[1], L Li[1], A Babalmorad[1], S Bagby[2], JJ Arcaroli[2,3], RJ Hansen[3,4], FA Valeriote[5], DL Gustafson[3,4], J Schaack[3,6], WA Messersmith[2,3] and DV LaBarbera[1,3]

Aberrant T-cell factor (TCF) transcription is implicated in the majority of colorectal cancers (CRCs). TCF transcription induces epithelial–mesenchymal transition (EMT), promoting a tumor-initiating cell (TIC) phenotype characterized by increased proliferation, multidrug resistance (MDR), invasion and metastasis. The data presented herein characterize topoisomerase IIα (TopoIIα) as a required component of TCF transcription promoting EMT. Using chromatin immunoprecipitation (ChIP) and protein co-immunoprecipitation (co-IP) studies, we show that TopoIIα forms protein–protein interactions with β-catenin and TCF4 and interacts with Wnt response elements (WREs) and promoters of direct target genes of TCF transcription, including: *MYC, vimentin, AXIN2* and *LEF1*. Moreover, both TopoIIα and TCF4 ChIP with the N-cadherin promoter, which is a new discovery indicating that TCF transcription may directly regulate N-cadherin expression. TopoIIα N-terminal ATP-competitive inhibitors, exemplified by the marine alkaloid neoamphimedine (neo), block TCF activity *in vitro* and *in vivo*. Neo effectively inhibits TopoIIα and TCF4 from binding WREs/promoter sites, whereas protein–protein interactions remain intact. Neo inhibition of TopoIIα-dependent TCF transcription also correlates with significant antitumor effects *in vitro* and *in vivo*, including the reversion of EMT, the loss of TIC-mediated clonogenic colony formation, and the loss of cell motility and invasion. Interestingly, non-ATP-competitive inhibitors of TopoIIα, etoposide and merbarone, were ineffective at preventing TopoIIα-dependent TCF transcription. Thus, we propose that TopoIIα participation in TCF transcription may convey a mechanism of MDR to conventional TopoIIα inhibitors. However, our results indicate that TopoIIα N-terminal ATP-binding sites remain conserved and available for drug targeting. This article defines a new strategy for targeted inhibition of TCF transcription that may lead to effective therapies for the treatment of CRC and potentially other Wnt-dependent cancers.

INTRODUCTION

The colon epithelium comprises tube-shaped glands known as the crypts of Lieberkühn.[1] The epithelial cells lining these crypts are highly ordered and segmented: the base contains stem cells that produce proliferating progenitor cells that are migratory and feed into the upper part of the crypt where they become differentiated and non-proliferating.[1,2] The Wnt signaling pathway, which controls T-cell factor/lymphoid enhancer binding factor (TCF/LEF) gene transcription, denoted throughout as TCF transcription, dominates this self-renewing process.[2–4] Under normal control adenomatous polyposis coli acts as a gatekeeper[3] of this pathway by regulating the fate of cytoplasmic β-catenin through transport and binding of the destruction complex, which includes: axis inhibition protein (AXIN), casein kinase 1 (CK1), protein phosphatase 2A (PP2A) and glycogen synthase kinase 3 (GSK3).[5] In the absence of Wnt signaling, β-catenin is marked for proteasomal degradation by the destruction complex. However, Wnt signals inhibit destruction, leading to β-catenin nuclear localization and activation of TCF transcription.[6] Mutations in adenomatous polyposis coli or β-catenin are early events that promote colorectal cancer (CRC) through constitutive activation of TCF transcription.[2,7] Such mutations allow for a proliferating progenitor cell phenotype in the upper crypt leading to polyp formation or dysplastic aberrant crypt foci.[2,3] Proto-oncogenic and tumor-suppressor mutations in genes such as KRAS and p53 cause adenomas and then carcinomas.[3,7,8] Aberrant TCF transcription is implicated in the vast majority of all CRCs, including familial adenomatous polyposis as well as 80% of sporadic CRC.[3]

Epithelial–mesenchymal transition (EMT) is a reversible process essential for embryonic development and wound healing.[9,10] EMT allows cells to transition between adherent (epithelial) or mobile (mesenchymal) phenotypes. EMT is characterized by loss of expression of epithelial biomarkers such as E-cadherin and Zonula Occludens-1 (ZO-1) with concomitant re-expression of mesenchymal biomarkers such as vimentin and Slug.[10,11] These changes in expression and other signaling events lead to the loss of tight cell adherent junctions and reorganization of the cytoskeleton, promoting the motile and invasive phenotype that is also resistant to apoptosis.[12] Aberrant EMT is implicated in some of the most prominent human diseases, including tumor progression and metastasis.[13,14] TCF activity and cues from the microenvironment stimulate EMT to acquire an invasive phenotype that can promote metastatic dissemination.[15–18] TCF-mediated EMT also promotes biologically distinct populations of tumor-initiating cells (TICs) with

[1]Department of Pharmaceutical Sciences, Skaggs School of Pharmacy and Pharmaceutical Sciences, University of Colorado Anschutz Medical Campus, Aurora, CO, USA; [2]Department of Immunology and Microbiology, University of Colorado Anschutz Medical Campus, Aurora, CO, USA; [3]Division of Medical Oncology, School of Medicine, University of Colorado Anschutz Medical Campus, Aurora, CO, USA; [4]University of Colorado Cancer Center, University of Colorado Anschutz Medical Campus, Aurora, CO, USA; [5]Colorado State University, Flint Animal Cancer Center, Fort Collins, CO, USA and [6]Josephine Ford Cancer Center, Henry Ford Health Systems, Detroit, MI, USA. Correspondence: Professor DV LaBarbera, Department of Pharmaceutical Sciences, Skaggs School of Pharmacy and Pharmaceutical Sciences, University of Colorado Anschutz Medical Campus, Aurora, CO 80045, USA.
Email: Daniel.LaBarbera@ucdenver.edu

'stem cell-like' properties, termed CRC stem cells (CRCSC).[19–23] Hence, targeting EMT as a therapeutic strategy may result in more effective treatments and better outcomes for CRC patients. Although our collective knowledge of the biology of EMT is immense, significant challenges remain in identifying viable targets for therapeutic development.

The multicellular tumor spheroid model (MCTS) is well established as an effective model for cancer drug discovery, which can be used to incorporate important components affecting EMT such as the tumor microenvironment (for example, extracellular matrix).[24] Previously, we developed a MCTS model of triple-negative breast cancer EMT suitable for high-throughput screening drug discovery.[25] Similarly, we have developed a model that utilizes vimentin promoter (VimPro) driven enhanced green fluoresecent protein (GFP) stably engineered as a surrogate reporter of the mesenchymal phenotype in SW620 MCTS CRC. We chose vimentin because it is a well-characterized biomarker that has a functional role in the mesenchymal phenotype and has been shown to be predictive for lymph node metastasis and poor prognosis in CRC.[26–28] Using this model, we identified neoamphimedine (neo) (Figure 1a), a marine alkaloid from Xestospongia sp. that significantly downregulates vimentin expression. Neo was first identified by Ireland and Barrows to be an inhibitor of topoisomerase IIα (TopoIIα).[29,30] TopoIIα is an important drug target for the treatment of many types of cancer because of its ability to modulate the topology of DNA, making it an essential enzyme for cell cycle progression.[31] Unlike conventional TopoIIα drugs used in the clinic (for example, etoposide), neo does not poison TopoIIα by stabilizing enzyme-DNA complexes.[29] Instead, we have shown that neo is an ATP-competitive inhibitor of the N-terminal ATPase domain, eliciting anticancer effects.[32,33] Furthermore, this mode of inhibition appears to overcome significant multidrug resistance (MDR) observed with TopoIIα poisons.[32] Herein, we describe and characterize TopoIIα as a DNA-binding partner for the TCF transcription complex that promotes EMT and the malignant phenotype. We show that ATP-competitive inhibitors can block TopoIIα-dependent TCF transcription, reversing EMT. These effects correlate with a significant loss of CRCSC stemness and invasive potential. Finally, we also show that inhibiting TopoIIα-dependent TCF transcription in vivo results in diminished tumor growth. Taken together, our results indicate a role for TopoIIα-dependent TCF transcription as a master regulator of EMT in CRC.

RESULTS

TopoIIα-dependent TCF transcription regulates EMT in CRC

SW620 CRC cells stably transduced with VimPro-GFP and Nuclight-Red were cultured as MCTS arrayed in 96-well plates as single uniform spheroids. This live multiplex assay allows us to monitor the modulation of EMT and cytotoxic effects in real time without fixing or adding reagents to the system. SW620 MCTS treated with neo exhibited significant downregulation of VimPro-GFP expression in a dose- and time-dependent manner over 72 h compared with 1% dimethylsulfoxide (DMSO) vehicle and 10% TritonX-100, a control used to indicate MCTS cell death (Figures 1b and c). As we have previously characterized neo as an N-terminal ATP-competitive inhibitor of TopoIIα,[32] we also tested a clinically used TopoIIα drug, etoposide, for its ability to downregulate vimentin expression. Etoposide and other TopoIIα poisons act through binding to the C-terminus of TopoIIα and stabilizing a transient covalent complex with DNA, known as the cleavage complex.[31] Even at a high concentration of 50 μM, etoposide had no effect on VimPro-GFP expression (Figures 1b and c). We also examined vimentin protein expression by fixing and staining SW620 MCTS after neo or etoposide treatment (Figure 1d). Like VimPro-GFP expression, neo significantly downregulated vimentin protein expression, whereas etoposide had no apparent effect. Loss of E-cadherin with
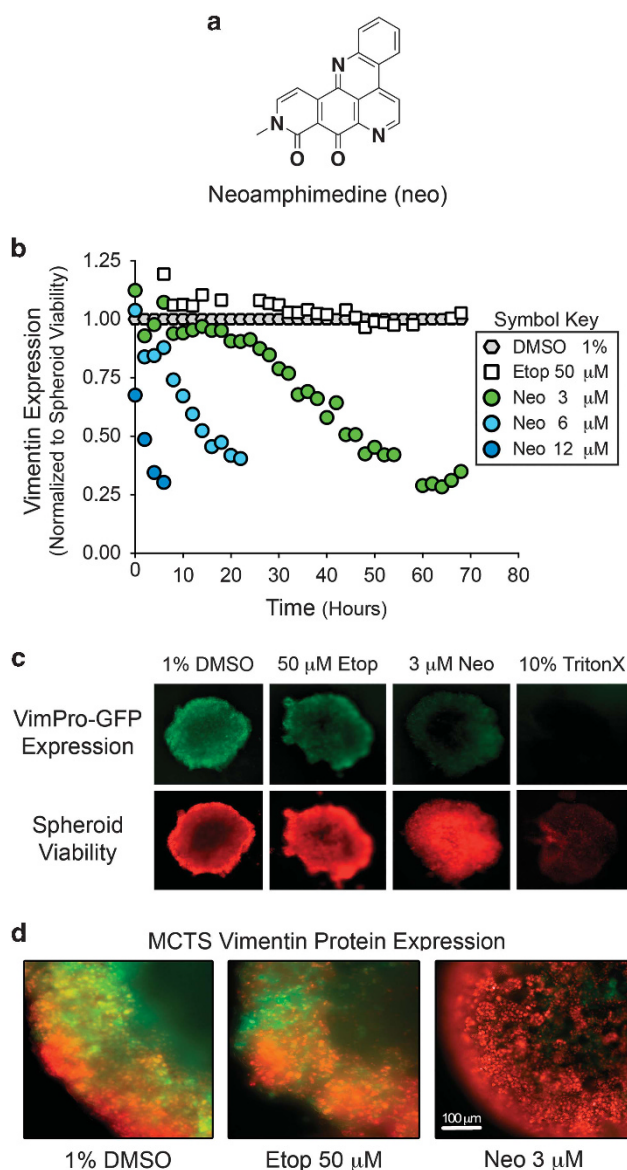

Figure 1. Neo downregulates vimentin promoter activity and protein expression in SW620 MCTS. (**a**) The chemical structure of neo. (**b**) SW620 cells transduced with VimPro-GFP and Nuclight-Red (nuclear restricted red fluorescent protein (RFP)) were plated as MCTS in 96-well plates. Vimentin promoter regulated GFP expression was normalized to viable cells using Nuclight-Red every 2 h for a 72-h drug treatment period. Data are shown as the mean of three replicates compared with DMSO. Neo downregulated vimentin promoter activity in live SW620 MCTS in a time- and dose-dependent manner, whereas etoposide (C-terminus binding TopoIIα poison) did not. (**c**) Representative IncuCyte (4x objective) 72-h images indicating that neo downregulated vimentin expression (GFP) without inducing significant MCTS cell death (RFP). Etoposide had no significant effect on GFP or RFP, whereas TritonX-100 downregulated both GFP and RFP because of MCTS cell death. (**d**) Close up images of SW620 spheroids treated with DMSO, 50 μM etoposide, or 3 μM neo for 72 h. Spheroids were fixed and stained for vimentin protein expression (GFP), and live cell nuclei were labeled with Nuclight-Red (RFP). Neo downregulated vimentin protein expression in SW620 MCTS, whereas etoposide did not. Images were captured using a 20x long-WD objective with a PerkinElmer Operetta High Content Screening System, each maximum projection image was projected from 10 Z-planes, with 1 μm distance between Z-planes.

concomitant upregulation of vimentin, SNAI2 (Slug), and zinc-finger E-box binding homeobox 1 (ZEB1) expression correlates with increased metastatic potential, tumor recurrence and overall poor prognosis in CRC patients.[34] In addition, decreased expression of E-cadherin and ZO-1 in CRC correlates with liver metastasis.[35] To further assess neo's effect on EMT, we conducted western blot analysis using CRC MCTS after 72-h treatments with neo (Figure 2a). The results indicate that neo downregulated mesenchymal markers,

including: vimentin, Slug, ZEB1 and the proto-oncogene product MYC (c-Myc). Moreover, neo treatment also resulted in the upregulation of epithelial markers ZO-1 and E-cadherin.

To further validate Topollα as the target of interest, we treated SW620 MCTS with another N-terminal ATP-competitive inhibitor of Topollα, benzothiazole amino purine (BAP-1), reported by Novartis (Cambridge, MA, USA) (Supplementary Figure S1) (see Supplementary Figure S1 and Daumar et al.[36] for BAP-1 preparation).[37] BAP-1 mimics neo's effects on EMT by downregulating vimentin, Slug, ZEB1 and c-Myc. Our next goal was to determine if neo's anticancer effects resulted from inhibiting an alternative target other than Topollα. Protein kinases have emerged as the predominant factors promoting human cancers.[38,39] Thus, we screened neo against a panel of 156 kinase enzymes implicated in carcinogenesis using the KinaseSeeker assay.[40] The kinase inhibition data indicate that neo is not a potent kinase inhibitor (Supplementary Figure S2). Taken together, the data in Figure 1, Supplementary Figure S1 support Topollα as a major cellular target of neo.

Neo inhibition of Topollα resulted in the downregulation of vimentin, Slug, ZEB1 and c-Myc, which are direct downstream targets of TCF transcription.[16,28] Therefore, we hypothesized that Topollα affects EMT through a TCF-dependent mechanism. To test this hypothesis, we conducted inhibition studies utilizing the well-characterized TOPflash (TOP) reporter.[41] We subcloned TOP into a lentiviral backbone and stably transduced this vector into DLD1, HCT116, SW480 and SW620 cells and used these cells to generate MCTS. After 72-h treatment with neo, we observed significant downregulation of TCF activity in all the CRC MCTS compared with the DMSO controls (Figure 2b). Using HCT116 MCTS, we determined neo's dose response for inhibiting Topollα-dependent TCF transcription ($IC_{50} = 3.5$ μM) (Figure 2c). Similarly, neo also induced MCTS cytotoxicity ($IC_{50} = 4.2$ μM). To confirm that neo's effect on TCF transcription was not a result of cell death, we conducted a time course study for both cytotoxicity (fluorescence) and TCF activity (luminescence) (Figure 2d). This experiment revealed that neo first inhibited Topollα-dependent TCF transcription over a time course of 20 h (Figure 2d inset) and then cytotoxicity ensued with significant cell death occurring at 56 h. In addition to MCTS models of CRC, neo displays potent nM cytotoxicity in a panel of 32 CRC cell lines cultured as monolayers (Supplementary Figure S3). Like neo, it is important to emphasize that most anticancer agents display more potent cytotoxicity in two-dimensional cell culture models compared with three-dimensional (3D) MCTS.[42]
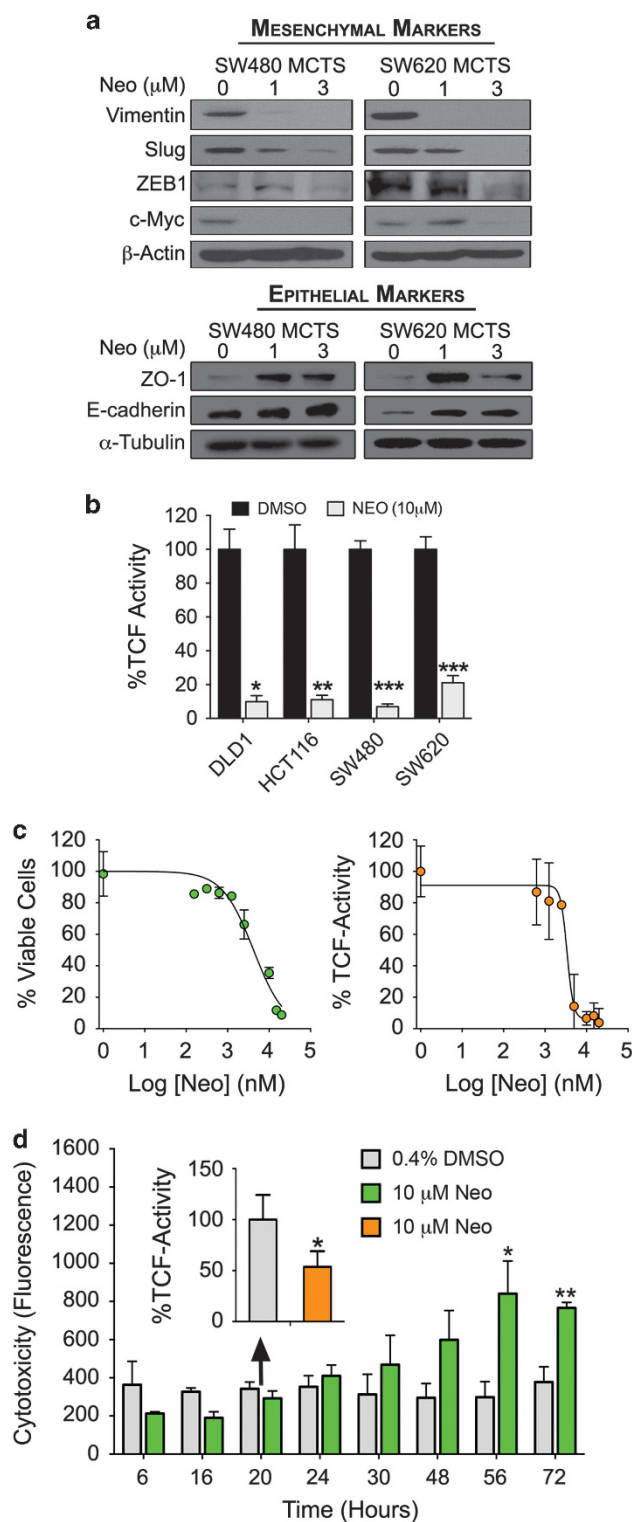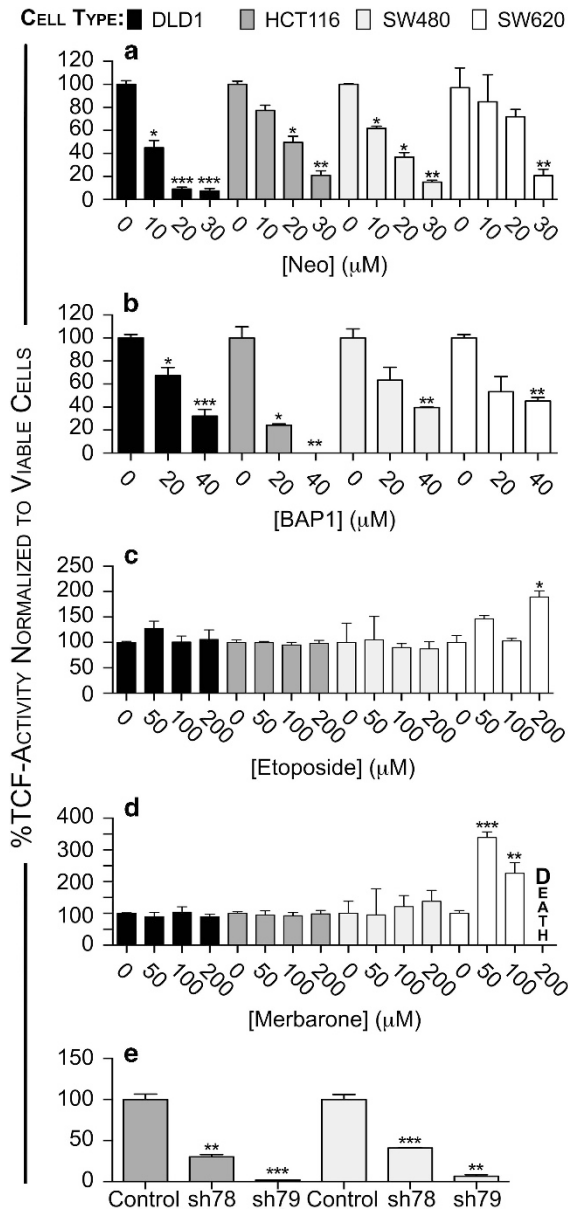

Figure 2. ATP-competitive inhibition of Topollα-dependent TCF transcription correlates with the reversion of EMT and cell death in MCTS. (**a**) MCTS western blot indicates that neo reverted EMT, evidenced by the downregulation of a panel of key mesenchymal genes (including the proto-oncogene c-Myc) and upregulation of key epithelial genes ZO-1 and E-cadherin. (**b**) Neo significantly inhibited TCF transcription in a panel of CRC MCTS stably transduced with the TOPflash reporter. (**c**) HCT116 MCTS 72-h cytotoxicity dose response for neo was measured using the Celltox Green assay (left, cytotoxicity $IC_{50} = 4.2$ μM), and a dose response for neo inhibition of TCF transcription was measured using HCT116 MCTS stably transduced with the TOPflash reporter (right, TCF activity inhibition $IC_{50} = 3.5$ μM). (**d**) A time course study for cytotoxicity and TCF transcription indicates that neo induced significant cytotoxicity at $t = 56$ h compared with DMSO. Neo significantly inhibited TCF activity at or before $t = 20$ h shown as an inset indicated with a black arrow. Therefore, neo inhibition of Topollα-dependent TCF transcription is an early event leading to MCTS cell death. Bar graphs indicate average ± s.d. The t-test statistical analysis was used to determine significance, where *$P \leqslant 0.05$, **$P \leqslant 0.01$ and ***$P \leqslant 0.001$.

ATP-competitive inhibitors of Topolla block Topolla-dependent TCF transcription

To further assess the mechanism of action resulting in the inhibition of Topolla-dependent TCF transcription, we conducted inhibition studies using three different classes of Topolla inhibitors, including: ATP-competitive inhibitors (neo and BAP-1), a general catalytic inhibitor (merbarone) and a poison (etoposide). For this study, we utilized a simplified two-dimensional cell-based model using relative

Figure 3. ATP-competitive inhibition of Topolla downregulates TCF transcription in a panel of four colon cancer cells cultured as monolayers. (**a**) Neo inhibits TCF transcription in a dose-dependent manner. (**b**) BAP-1 inhibits TCF transcription in a dose-dependent manner. (**c**) Etoposide does not inhibit TCF transcription. (**d**) Merbarone does not inhibit TCF transcription. (**e**) shRNA knockdown of Topolla recapitulated neo's effects in downregulating TCF transcription. Experiments with drug treatment were optimized using relatively high doses and short treatment times of 6 h. The %TOP activity for each experiment was normalized to viable cell protein concentration. Bar graphs indicate average ± s.d. The t-test statistical analysis was used to determine significance, where *$P \leqslant 0.05$, **$P \leqslant 0.01$ and ***$P \leqslant 0.001$.

high concentrations of drug in order to measure inhibition over a 6 h time course using DLD1, HCT116, SW480 and SW620 cells transfected with TOP (Figure 3). Neo and BAP-1 blocked TCF activity in a dose-dependent manner, and neo displayed more potent inhibition of Topolla-dependent TCF transcription (Figures 3a and b). Etoposide had no inhibition of TCF activity over a concentration range between 50 and 200 μM (Figure 3c), which is consistent with the data shown in Figure 1. Similarly, merbarone was ineffective at inhibiting Topolla-dependent TCF transcription, and significantly upregulated TCF activity or caused complete cell death in SW620 cells (Figure 3d). To further characterize Topolla as a required component of TCF transcription, we stably knocked down Topolla using short hairpin RNA (shRNA; sh78 and sh79) in HCT116 and SW480 cells followed by transfecting the TOP reporter. Compared with scrambled control shRNA, sh78 and sh79 significantly downregulated Topolla-dependent TCF transcription, recapitulating neo's inhibitory effects (Figure 3e). The level of TCF transcription inhibition was correlated with the level of Topolla knockdown by western blot quantification. Taken together, the data in Figure 3 indicate that Topolla is an important component of TCF transcription. Moreover, ATP-competitive inhibition of Topolla proves to be an effective mode of action to block Topolla-dependent TCF transcription.

Topolla functions as a DNA-binding partner for the TCF complex

We hypothesized that Topolla participates in the TCF complex by forming protein–protein interactions via its C-terminus. Consistent with our hypothesis, Huang et al.[43] reported that Topolla co-immunoprecipitated (co-IP) with TCF4 and β-catenin using DLD1 cells, and they identified that protein–protein interactions occur via the C-terminus of Topolla. To test our hypothesis, we conducted co-IP studies using SW620 cells (Figure 4a) as well as DLD1 and HCT116 cells (Supplementary Figure S5) that were treated with or without neo. Our goal was to identify protein–protein interactions and to determine if neo could block these interactions. The data in Figure 4a and Supplementary Figure S5 demonstrate that Topolla formed robust interactions with β-catenin as well as with TCF4. However, neo treatment did not prevent these protein–protein interactions from occurring.

TCF proteins bind to consensus sequences known as Wnt-responsive elements (WREs).[44] To determine if Topolla functions as a DNA-binding partner for the TCF complex, we conducted chromatin immunoprecipitation (ChIP) studies with Topolla and TCF4.[45] Indeed, Topolla and TCF4 bind to known TCF target gene WRE/promoter sites, including: *AXIN2*, *MYC*, *LEF1* and *vimentin* (Figure 4b), and neo inhibits their binding to these sites. Moreover, we conducted ChIP analysis using the N-cadherin promoter and found that both Topolla and TCF4 bind to this promoter and neo can also significantly inhibit these protein–DNA interactions. N-cadherin expression has been shown to be upregulated because of TCF transcription, promoting EMT.[46–48] The direct binding interactions we observed with both Topolla and TCF4 are novel discoveries, indicating that Topolla-dependent TCF transcription may directly regulate N-cadherin gene expression, which is a key EMT effector.[14]

Topolla-dependent TCF transcription promotes a malignant phenotype in CRC

Wnt/TCF transcription has been reported to promote a CRCSC phenotype, and both EMT and CRCSC phenotypes are associated because of overlapping gene expression.[14,19,23,49,50] Therefore, it is likely that inhibiting Topolla-dependent TCF transcription will also suppress CRCSCs. To test this, we utilized the clonogenic assay, which is a surrogate measure of the stemness of TICs or cancer stem cells.[49,51] We found that inhibition of Topolla either by shRNA or by neo inhibited clonogenic colony formation
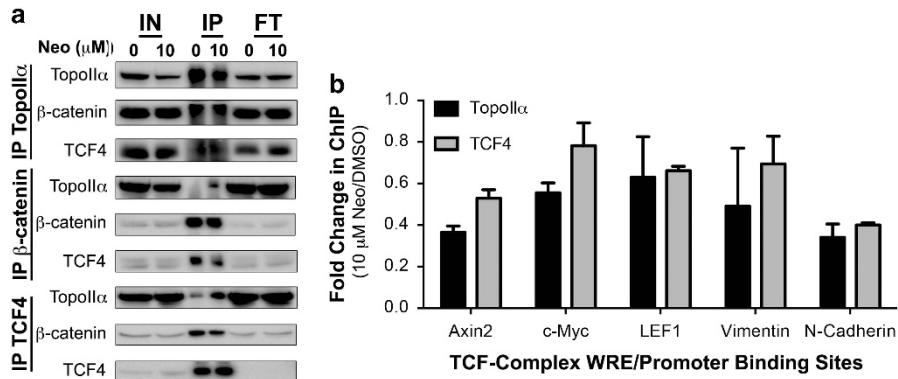
Figure 4. TopoIIα functions as a DNA-binding partner for the TCF complex. (**a**) Co-IP studies were performed with TopoIIα, β-catenin and TCF4 using SW620 cells treated with neo (10 μM) or DMSO for 6 h. Western blot from nuclear lysates used for IP is denoted as input (IN) before IP or flow through (FT) after IP. The results indicate that TopoIIα forms protein–protein interactions with β-catenin and TCF4 in nuclei, and that neo treatment does not prevent these interactions. (**b**) Using SW620 cells and the same neo treatment conditions for co-IP, ChIP studies were performed to determine protein–DNA interactions. TopoIIα and TCF4 bind to WREs/promoters as indicated and neo significantly inhibits this protein–DNA binding interaction. All experiments were conducted at least two times. QPCR from ChIP was conducted with duplicates. Bar graph indicates average ± s.d.
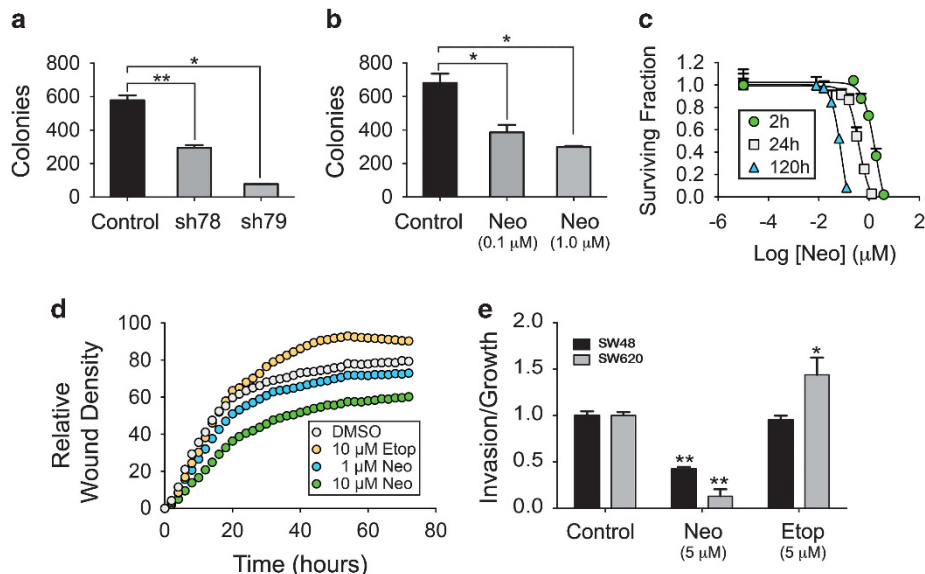
Figure 5. TopoIIα-dependent TCF transcription regulates CRCSC stemness and cell motility in CRC. (**a**) SW620 cells transduced with TopoIIα shRNA displayed significantly diminished CRCSC mediated colony formation compared with the scrambled control (Scr). (**b**) Pretreatment of SW620 cells for 24 h with Neo, as indicated, significantly reduced the number of colonies formed. (**c**) Continuous exposure of HCT116 cells for three different periods of time (2, 24 and 120 h) with various concentrations of neo followed by clonogenic analysis demonstrated that inhibition of colony formation by neo was both concentration and exposure time dependent. (**d**) Neo treatments in HCT116 cells inhibited wound healing migration in a dose-dependent manner compared with DMSO, whereas etoposide increased migration (data presented as the average of six replicates). (**e**) CRC MCTS treated with neo or etoposide, as indicated for 72 h, were dissociated and either plated into invasion chambers or in 96-well plates to assess invasion and proliferation, respectively. The invasive potential normalized to proliferation indicated that neo inhibited invasion independent of cell growth. Etoposide either had no effect or increased the invasion potential ($n = 4$). ImageJ analysis was used to quantify CRC colony formation and the t-test analysis was used to assess statistical significance, where $*P \leqslant 0.05$, $**P \leqslant 0.01$. Bar and line graphs indicate average ± s.d.

(Figures 5a and b). Pretreating cells with 100 nM neo for 24 h before plating the clonogenic assay was sufficient to reduce colony formation by approximately 50% over 10 days. We then investigated the time–survival relationships with various durations of pre-exposure to neo against HCT116 cells (Figure 5c). For a 2, 24 and 120-h exposures at least 2.6, 0.5 and 0.1 μM of neo were required to obtain a 90% clonogenic killing, respectively.

Inherent to the EMT positive TIC phenotype is increased motility. Thus, we assessed neo's ability to prevent cell migration

and invasion compared with DMSO and etoposide (Figures 5d and e). Neo significantly inhibited cell migration in a dose-dependent manner. By stark contrast, etoposide increased the migration potential. Next, we conducted invasion assays using cells harvested from SW48 and SW620 MCTS that were treated with neo or etoposide. After treatment, MCTS were dissociated into single-cell suspensions and seeded into either 96-well invasion chambers coated with Matrigel or into standard 96-well tissue culture plates to assess proliferation (Figure 5e). Importantly, no

further treatment was done after dissociating the MCTS or during the invasion studies. The invasive potential normalized to cell proliferation indicates that neo significantly inhibits invasion. Like migration, etoposide increases the invasive potential of SW620 cells and had no effect on SW48 cells.

TopoIIα-dependent TCF transcription promotes tumor growth *in vivo*

To further validate our *in vitro* findings, we conducted *in vivo* tumor growth studies using SW620 cells stably transduced with the TOPflash reporter, allowing us to monitor TopoIIα-dependent TCF activity by IVIS imaging. First, we administered neo (25 mg/kg) by intraperitoneal or intravenous tail vain injection similar to the protocol used by Marshall *et al.*[29] However, we observed no

antitumor activity. This result is most likely due to pharmacokinetic and distribution issues with neo. As shown in Supplementary Figure S6, neo is metabolized substantially by liver microsomes and pharmacokinetic data in rats show less metabolism of neo than mice, which reach a C_{max} following intravenous administration of 1.4 mg/kg, approximately 1 μM (315 ng/ml). This concentration is substantially below the 10 μM shown to significantly decrease TCF activity by TOP in cell culture after 6-h exposure (Figure 3a), and even with a linear extrapolation between mice dosed at 25 mg/kg and rats dosed at 1.4 mg/kg the plasma concentration in mice would be estimated to reach a C_{max} of 17.9 μM and remain above 10 μM for < 2 h. Next, we repeated the tumor growth study administering neo by intratumoral injection. Neo downregulated TCF transcription and tumor volume in a dose-dependent manner over 22 days (Figures 6a and b). In addition,
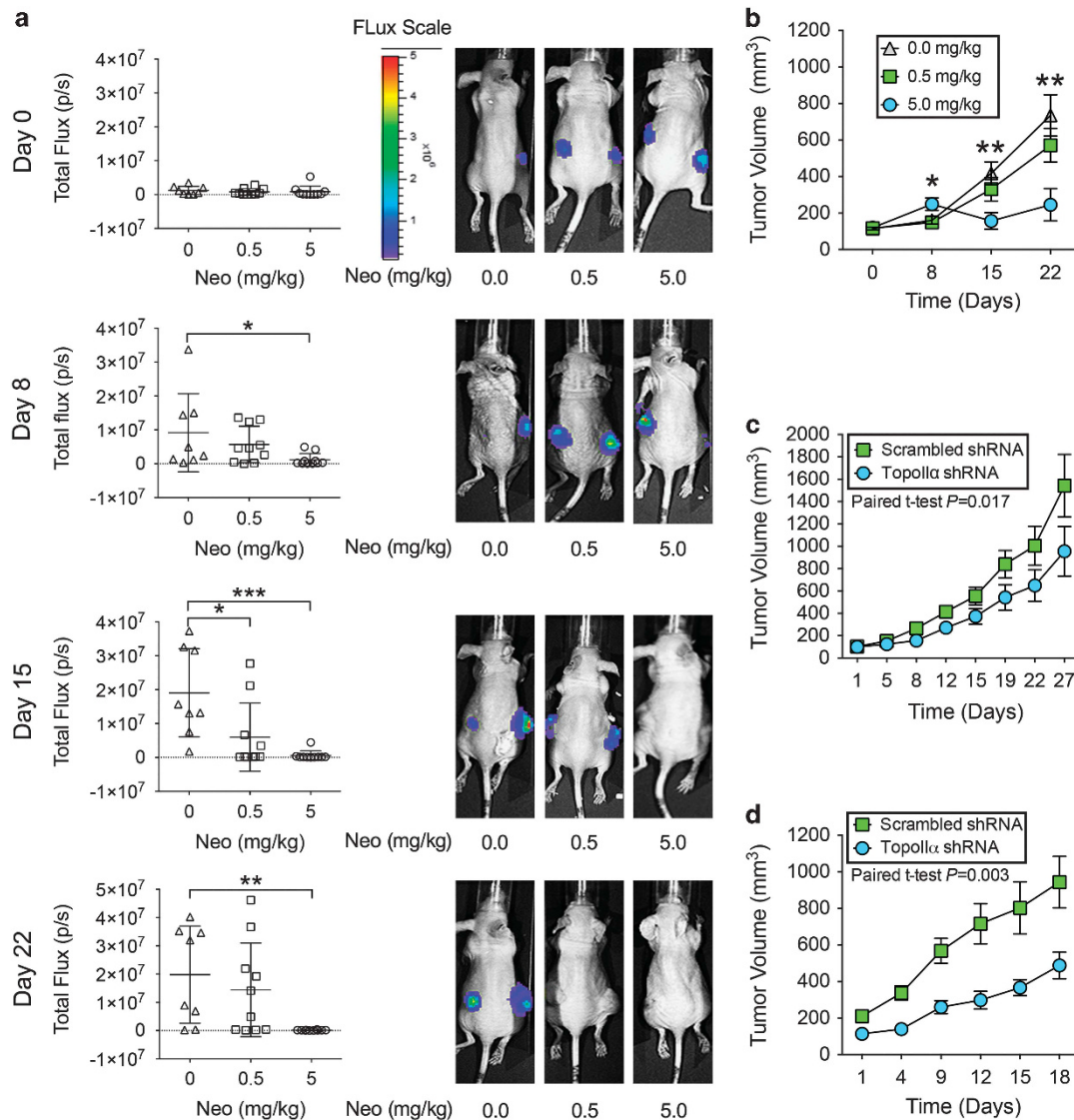
Figure 6. Neo inhibits TopoIIα-dependent TCF transcription and tumor growth in SW620 xenografts. (**a**) Neo was administered intratumoral (i.t.) 1× per week over 22 days. Within 15 days of neo treatment, measured by IVIS imaging, we observed a significant loss of TOPflash TCF transcriptional activity in the 0.5 mg/kg treatment group and complete loss of TCF activity in the 5 mg/kg treatment group, *t*-test where *P ⩽ 0.05, **P ⩽ 0.01, ***P ⩽ 0.001. Scatter plots indicate average ± s.d. (**b**) SW620 xenografts were treated with neo via i.t. 1× per week as indicated for 22 days. Neo inhibited tumor growth in a dose-dependent manner compared with the vehicle control and the 5 mg/kg treatment group significantly inhibited tumor growth by day 15 and prevented tumor growth for the remainder of the study compared with the vehicle group, *P ⩽ 0.05, **P ⩽ 0.01. (**c**) SW620 cells and (**d**) SW480 cells stably transduced with scrambled or TopoIIα shRNA (50% and 90% knockdown for SW620 and SW480, respectively) were used to generate tumor xenografts in athymic nude mice. Paired *t*-test analysis indicated that the TopoIIα knockdown group had significantly diminished tumor volumes compared with the scrambled shRNA control group. In addition, the magnitude of TopoIIα knockdown correlated with significance of tumor inhibition. Line graphs indicate average ± s.e.m.
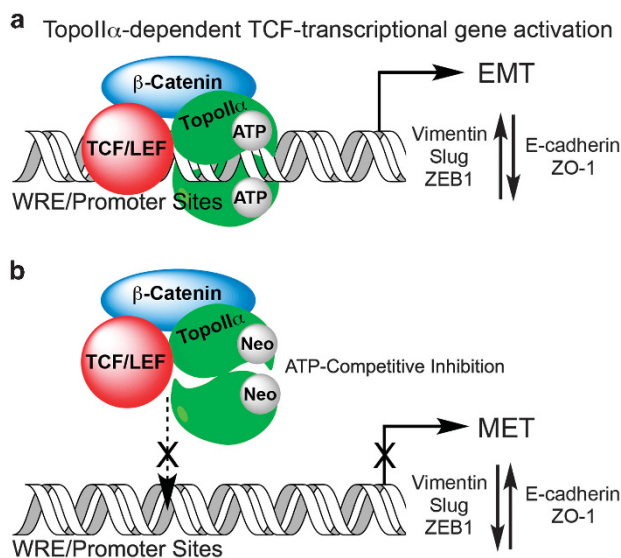
knockdown of Topollα expression by 50% (SW620) and 90% (SW480) also significantly reduced tumor volume (Figures 6c and d). These animal studies further validate Topollα-dependent TCF transcription as a mechanism promoting tumor growth, which can be inhibited with ATP-competitive inhibitors of Topollα.

DISCUSSION

Since the discovery of topoisomerases in 1971,[52] these ubiquitous enzymes have proved to be essential for regulating DNA topology, including: supercoiling/relaxation, knotting/unknotting and catenation/decatenation. In particular, Topollα has emerged as a master regulator of the cell cycle for its role in decatenating chromatin DNA, which is a checkpoint required for G2-M phase progression.[53] Moreover, the range of important biological functions and protein–protein interactions for Topollα is ever expanding.[54] The data presented herein define Topollα as a DNA-binding partner of the TCF transcription complex. Using Topollα inhibitors and shRNA, we determined that Topollα is a required component of TCF transcription. Interestingly, only ATP-competitive inhibitors of Topollα, exemplified by neo, prevent Topollα-dependent TCF transcription. TCF/LEF members have modest DNA-binding affinity and specificity.[55,56] To dynamically regulate gene expression TCF/LEFs also recruit other DNA-binding factors to regulate their affinity to WREs/promoter sites.[55,56] As Topollα is a key enzyme regulating DNA topology, we hypothesized that it functions as a DNA-binding protein for the TCF complex. Indeed, the ChIP data in Figure 4b indicate that Topollα binds to WRE/promoter sites and that DNA-binding by both Topollα and TCF4 can be inhibited by neo.

As a result of our findings, we conclude that Topollα functions as a DNA-binding partner for the TCF complex interacting with β-catenin, TCF4 and DNA through the C-terminus of Topollα (Figure 7a). Further, we hypothesize that ATP is required for Topollα-dependent

TCF transcription and that N-terminal ATP-binding sites are conserved and available when Topollα participates in the TCF complex, allowing for ATP-competitive inhibition by neo (Figure 7b). The requirement of ATP is substantiated by the fact that neo prevents Topollα and TCF4 from binding to WRE/promoter sites, which in turn may decrease the entire TCF complex binding affinity preventing transcription. Bates et al.[57] recently proposed that the energy of ATP hydrolysis by Topollα is used to strengthen both Topollα homodimer protein–protein interactions and Topollα–DNA interactions by inducing favorable binding conformations, which is in agreement with our findings and hypothesis. Although a mechanism of action requiring ATP hydrolysis may be an Achilles heel to drug resistance with ATP-competitive inhibitors, the participation of Topollα in the TCF protein complex may conversely be a mechanism of MDR for other Topollα inhibitors such as etoposide and merbarone. MDR is a major problem associated with the existing clinically used Topollα inhibitors,[58] including substrates of the MDR efflux pump[58] or through alterations in Topollα structure[59] like those that are likely to arise from Topollα participation in the TCF complex. Recently, we reported that neo can overcome MDR because of alterations in Topollα where etoposide, doxorubicin and ICRF-193 were ineffective.[32]

Drug discovery against the Wnt/TCF pathway has been hampered by significant challenges in identifying druggable targets.[59] This report validates Topollα-dependent TCF transcription as a druggable target and demonstrates that inhibition of Topollα-dependent TCF transcription is an early event that correlates with significant antitumor effects and may ultimately prevent invasion and metastasis. Specifically, we show that neo induces the reversion of EMT by downregulating vimentin, Slug, ZEB1 and c-Myc expression with concomitant upregulation of E-cadherin and ZO-1. Importantly, both E-cadherin and ZO-1 are negatively regulated by Slug and ZEB1,[14] which is in agreement with our findings. Furthermore, TCF transcription directly regulates vimentin, Slug and ZEB1,[16,28] promoting EMT during CRC tumor progression and metastasis.[15–18] Thus, Topollα-dependent TCF transcription may function as a master regulator of EMT by regulating key EMT effectors. Reversion of EMT by a single agent, neo, through the blockade of TCF transcription correlates with the loss of malignant phenotype and significantly inhibited tumor growth in mice.

In conclusion, Topollα is highly expressed in CRC, particularly in metastatic or recurring CRC.[60,61] This article defines a role for Topollα as a DNA-binding factor required for TCF transcription that promotes EMT and the malignant phenotype in CRC. Moreover, Topollα is a versatile drug target that may emerge not only as a master regulator of the cell cycle but also to function as a master regulator of gene expression by participating as an ATP-dependent DNA-binding partner in an array of gene transcriptional machinery. Thus, ATP-competitive inhibitors of Topollα may be effective targeted therapies for the treatment of CRC and potentially many other types of cancer.

MATERIALS AND METHODS

Cell culture

Cell lines were cultured as monolayers or MCTS using RPMI-1640 containing 5% fetal bovine serum. MCTS were generated using our previously reported method[25] by seeding 20 000 cells per well into un-coated 96-well U-bottom Ultra Low Attachment Microplates (Corning Inc., Corning, NY, USA). Four days after plating, MCTS were treated with compounds in 25 μl of medium containing 5% Matrigel for 72 h.

VimPro-GFP reporter, protein staining, and 3D western blots with MCTS

SW620 cells were transduced with Nuclight-Red virus (Essen BioSciences, Ann Arbor, MI, USA) and selected with Zeocin (200 μg/ml), and then transduced with pCDH-VimPro-GFP-EF1-puro virus and selected with puromycin at 4 μg/ml.

Figure 7. Model for Topollα-dependent TCF transcription and inhibition with ATP-competitive inhibitors. (**a**) Topollα forms C-terminus protein–protein interactions with β-catenin and TCF4, and functions as a DNA-binding protein for the TCF complex, which is required for WRE/promoter activation, inducing mesenchymal gene expression and EMT. (**b**) ATP-competitive inhibitors of Topollα, such as neo, bind to N-terminal ATP sites, preventing Topollα-TCF complex protein–DNA interactions, which in turn leads to the downregulation of mesenchynal gene expression with concomitant upregulation of epithelial genes, promoting mesenchymal–epithelial transition (MET).

The dual fluorescently labeled cells were used to generate 3D MCTS and treated as described. MCTS images were recorded every 2 h over a 72-h period using an IncuCyte ZOOM content imaging system (Essen BioSciences) (n = 3). SW620 cells transduced with Nuclight-Red were used to generate 3D MCTS and treated as described. Protein staining and western blot analyses were done as previously reported.[25] MCTS were imaged using an Operetta System (PerkinElmer, Waltham, MA, USA). All western blots were replicated twice.

MCTS cytotoxicity

The CellTox Green assay (Promega, Madison, WI, USA) was used with 3D MCTS to measure spheroid death (n = 3). In all, 0.1% CellTox Green was included in each well at the time of neo dosing. In total, 10% lysis solution was used as a cell death control. Fluorescence was measured at various time points with 485–510 nm excitation and 520–530 nm emission.

TCF reporter assay in monolayer cell culture and MCTS

TOPflash (Millipore, Billerica, MA, USA) was used to evaluate TCF transcriptional activity in CRC cells. A total of 10 000 cells per well were plated into 96-well plates and transfected with TransLT1 reagent (Mirus, Madison, WI, USA). After 24 h, medium was replaced and cells were treated with compounds as indicated for 6 h. Next, cells were washed with phosphate-buffered saline (PBS) and a 1:1 ratio of PBS: One-Glo luciferase reagent (Promega) was added and the luminescence was detected within 10 min. The experiment was repeated to measure viable cell protein concentration after compound treatment, which was used to normalize TOPflash luminescence to obtain the %TCF activity. Stable engineered cells containing pCDH-TOPflash-luc-EF1-puro were used to generate MCTS arrayed in 96-well plates and treated with DMSO or 10 μM neo for 72 h. One-Glo and 3D-CellTiter-Glo (Promega) were used to determine the TCF reporter activity in viable cells from MCTS. Experiments were replicated twice (n = 3 for each replicate).

Co-immunoprecipitation

Cells were treated with DMSO or 10 μM neo for 6 h followed by generating cytoplasmic and nuclear lysates. In all, 100 μl of 1 mg/ml nuclear extract was saved and used as the input. IP was conducted with Dynabeads protein A IP Kit (ThermoScientific, Waltham, MA, USA). Briefly, 300 μg of lysate incubated with 1–2 μg of the IP antibody was rotated at 4 °C for 2 h. In total, 50 μl of beads were transferred to the preincubated antibody/lysate mixture followed by overnight incubation at 4 °C. The flowthrough was collected and the beads were washed 3× with PBST. Proteins were eluted with 20 μl of 50 mM glycine (pH = 2.8). Experiments were replicated twice.

Chromatin immunoprecipitation

The methods used for ChIP were previously published[62] and are detailed in the Supplementary Information Materials and methods section. Experiments were replicated twice (n = 2 for quantitative PCR).

Clonogenic assay

SW620 cells were plated to allow for 70% confluency within 24 h. Neo, BAP-1 and DMSO were then added to cells for 24 h as pretreatment. A total of 1000 viable cells per well were plated into a six-well plate and medium was changed 2× per week. After 10 days in culture, the medium was removed and cells colonies were washed with PBS and fixed with acetic acid:methanol (1:7 v-v) at room temperature for 5 min. The fixed colonies were stained with 0.5% (w/v) crystal violet in 25% (v/v) methanol solution for 2 h at room temperature. The stain was rinsed off with water and the plate was air dried at room temperature. Digital pictures were taken and the images were saved in greyscale (8-bit). Images were adjusted for threshold with ImageJ software (Bethesda, MD, USA), the area of analysis was circled and particles were analyzed by size (100–2000) and circularity (0.5–1). In addition to pretreatment, we conducted the clonogenic assay with continuous exposure to neo using the conditions described in Figure 5c. Experiments were replicated twice (n = 2 for each replicate).

Wound-healing and 3D invasion assays

HCT116 cells were plated in six replicates in an Essen Image Lock 96-well plate (Essen BioSciences) at 60 000 cells per well and were allowed to adhere for 24 h before scratching. Uniform wounds were made with the Essen WoundMaker before treatment. Wound closures were monitored with an Incycite ZOOM imaging system (Essen BioSciences) by acquiring images every 2 h over 72 h, and the relative wound density was analyzed using the Scratch Would Analysis module (n = 6). To measure MCTS, invasion cells were grown and treated in 3D as described. MCTS were collected, washed with PBS, and disassociated into single-cell suspension with 0.25% trypsin for 15 min at 37 °C. Cells were then neutralized with complete medium, pelleted by centrifugation and 12 500 viable cells in 50 μl of RPMI-1640 + 0.1% fetal bovine serum were plated using the Corning BioCoat Tumor Invasion System (Corning Inc.). A regular 96-well tissue culture plate was used as a growth control with the same number of cells plated at the same time. In all, 200 μl of RPMI-1640 + 10% fetal bovine serum was used as the chemoattractant in each basal chamber. After incubating for 72 h, medium was carefully removed from the apical chambers and the insert system was transferred into a second 96-square well-plate containing 200 μl per well of 4 μg/ml calcein AM in Hanks' Balanced Salt solution. The plate was incubated for 1 h at 37 °C and the fluorescence from invaded cells was measured (excitation 494 nm; emission 517 nm). The growth of the cells was measured by SRB assay.[33] The invaded cells to cell growth ratio was used to access the inhibition of invasion by neo or etoposide (n = 4).

Animal studies

Four- to 6-week-old female athymic nude mice (Harlan Laboratories, Denver, CO, USA) were anesthetized with isoflurane. Cells were injected at 2 500 000 cells per flank in 50 μl medium + 50 μl Matrigel into both flanks. Tumor size was evaluated twice per week by caliper using the following formula: tumor volume = (length × width^2) × 0.52. Mice were killed at the end of the experiment or when a single tumor volume reached 2000 mm^3 or combined tumors reached 3000 mm^3. All protocols used were approved by the Institutional Animal Care and Use Committee of the University of Colorado, Denver. SW620 cells stably transduced with TOPflash were used to generate the xenograft mouse model (n = 20) and animals were randomized into three groups (4 or 5 animals, 8 or 10 tumors per group) once the tumor volumes reached 100 mm^3. Animals without tumor or with tumor size > 200 mm^3 at the time of randomization were excluded from the study. Intratumoral injections were conducted once per week by slowly injecting to the center of each tumor with a 28-gauge insulin syringe while the mice were anesthetized with isoflurane. The day after intratumoral injection, mice were intraperitoneally injected with 3 mg D-luciferin (Gold Biotechnology, St Louis, MO, USA) in 200 μl PBS, and 5 min later mice were anesthetized with isoflurane for 5 min before imaged dorsally with the Xenogen IVIS 200 (PerkinElmer) imaging system. Bioluminescence activity in photons/s was measured using Living Image software (PerkinElmer). Tumor volume measurements were conducted blinded.

Statistical analysis

Data were subjected to unpaired two-tailed or paired Student's t-test statistical analysis using Prism (GraphPad Software Inc, La Jolla, CA, USA). All experiments were replicated two times (n = 3 for each replicate) unless otherwise described.

CONFLICT OF INTEREST

The authors declare no conflict of interest.

4998

REFERENCES

1 Reya T, Clevers H. Wnt signalling in stem cells and cancer. *Nature* 2005; **434**: 843–850.

2 van de Wetering M, Sancho E, Verweij C, de Lau W, Oving I, Hurlstone A *et al*. The β-catenin/TCF-4 complex imposes a crypt progenitor phenotype on colorectal cancer cells. *Cell* 2002; **111**: 241–250.

3 Kinzler KW, Vogelstein B. Lessons from hereditary colorectal cancer. *Cell* 1996; **87**: 159–170.

4 Batlle E, Henderson JT, Beghtel H, van den Born MM, Sancho E, Huls G *et al*. β-Catenin and TCF mediate cell positioning in the intestinal epithelium by controlling the expression of EphB/EphrinB. *Cell* 2002; **111**: 251–263.

5 Kimelman D, Xu W. β-Catenin destruction complex: insights and questions from a structural perspective. *Oncogene* 2006; **25**: 7482–7491.

6 Clevers H. Wnt/β-catenin signaling in development and disease. *Cell* 2006; **127**: 469–480.

7 Armaghany T, Wilson JD, Chu Q, Mills G. Genetic alterations in colorectal cancer. *Gastrointest Cancer Res* 2012; **5**: 19–27.

8 Fearon ER, Vogelstein B. A genetic model for colorectal tumorigenesis. *Cell* 1990; **61**: 759–767.

9 Kalluri R. EMT: when epithelial cells decide to become mesenchymal-like cells. *J Clin Invest* 2009; **119**: 1417–1419.

10 Hay ED. The mesenchymal cell, its role in the embryo, and the remarkable signaling mechanisms that create it. *Dev Dyn* 2005; **233**: 706–720.

11 Lee JM, Dedhar S, Kalluri R, Thompson EW. The epithelial-mesenchymal transition: new insights in signaling, development, and disease. *J Cell Biol* 2006; **172**: 973–981.

12 Gavert N, Ben-Ze'ev A. Epithelial-mesenchymal transition and the invasive potential of tumors. *Trends Mol Med* 2008; **14**: 199–209.

13 Thiery JP, Acloque H, Huang RY, Nieto MA. Epithelial-mesenchymal transitions in development and disease. *Cell* 2009; **139**: 871–890.

14 McDonald PC, Dedhar S. The role of epithelial–mesenchymal transition in cancer metastasis In: Regad T, Sayers TJ, Rees RC (eds), *Principles of Stem Cell Biology and Cancer* 1st edn. John Wiley & Sons, Ltd: West Sussex, UK, 2015, pp 101–121.

15 Xu Y, Pasche B. TGF-β signaling alterations and susceptibility to colorectal cancer. *Hum Mol Genet* 2007; **16**: R14–R20.

16 Sánchez-Tilló E, de Barrios O, Siles L, Cuatrecasas M, Castells A, Postigo A. β-Catenin/TCF4 complex induces the epithelial-to-mesenchymal transition (EMT)-activator ZEB1 to regulate tumor invasiveness. *Proc Natl Acad Sci USA* 2011; **108**: 19204–19209.

17 Medici D, Hay ED, Olsen BR. Snail and slug promote epithelial-mesenchymal transition through β-catenin-T-cell factor-4-dependent expression of transforming growth factor-β3. *Mol Biol Cell* 2008; **19**: 4875–4887.

18 Loboda A, Nebozhyn MV, Watters JW, Buser CA, Shaw PM, Huang PS *et al*. EMT is the dominant program in human colon cancer. *BMC Med Genomics* 2011; **4**: 1–10.

19 Polyak K, Weinberg RA. Transitions between epithelial and mesenchymal states: acquisition of malignant and stem cell traits. *Nat Rev Cancer* 2009; **9**: 265–273.

20 Zeki SS, Graham TA, Wright NA. Stem cells and their implications for colorectal cancer. *Nat Rev Gastroenterol Hepatol* 2011; **8**: 90–100.

21 Ricci-Vitiani L, Pagliuca A, Palio E, Zeuner A, De Maria R. Colon cancer stem cells. *Gut* 2011; **57**: 538–548.

22 Mani SA, Guo W, Liao MJ, Eaton EN, Ayyanan A, Zhou AY *et al*. The epithelial-mesenchymal transition generates cells with properties of stem cells. *Cell* 2008; **133**: 704–715.

23 Prabhu VV, El-Deiry WS, Finnberg N. Colon stem cells in colorectal cancer. In: Regad T, Sayers TJ, Rees RC (eds), *Principles of Stem Cell Biology and Cancer* 1st edn. John Wiley & Sons, Ltd: West Sussex, UK, 2015, pp 169–192.

24 LaBarbera DV, Reid BG, Yoo BH. The multicellular tumor spheroid model for high-throughput cancer drug discovery. *Expert Opin Drug Discov* 2012; **7**: 819–830.

25 Li Q, Chen C, Kapadia A, Zhou Q, Harper MK, Schaack J *et al*. 3D models of epithelial-mesenchymal transition in breast cancer metastasis: high-throughput screening assay development, validation, and pilot screen. *J Biomol Screen* 2011; **16**: 141–154.

26 Ivaska J, Pallari HM, Nevo J, Eriksson JE. Novel functions of vimentin in cell adhesion, migration, and signaling. *Exp Cell Res* 2007; **313**: 2050–2062.

27 Toiyama Y, Yasuda H, Saigusa S, Tanaka K, Inoue Y, Goel A *et al*. Increased expression of slug and vimentin as novel predictive biomarkers for lymph node metastasis and poor prognosis in colorectal cancer. *Carcinogenesis* 2013; **34**: 2548–2557.

28 Gilles C, Polette M, Mestdagt M, Nawrocki-Raby B, Ruggeri P, Birembaut P *et al*. Transactivation of vimentin by β-catenin in human breast cancer cells. *Cancer Res* 2003; **63**: 2658–2664.

29 Marshall KM, Matumoto SS, Holden JA, Concepcion GP, Tasdemir D, Ireland CM *et al*. The anti-neoplastic and novel topoisomerase II-mediated cytotoxicity of neoamphimedine, a marine pyridoacridine. *Biochem Pharmacol* 2003; **66**: 447–458.

30 Guzman FSD, Carte B, Troupe N, Faulkner DJ, Harper MK, Concepcion GP *et al*. Neoamphimidine: a new pyridoacridine topoisomerase II inhibitor which cantenates DNA. *J Org Chem* 1999; **64**: 1400–1402.

31 Nitiss JL. Targeting DNA topoisomerase II in cancer chemotherapy. *Nat Rev Cancer* 2009; **9**: 338–350.

32 Ponder J, Yoo BH, Abraham AD, Li Q, Ashley AK, Amerin CL *et al*. Neoamphimedine circumvents metnase-enhanced DNA topoisomerase IIα activity through ATP-competitive inhibition. *Mar Drugs* 2011; **9**: 2397–2408.

33 Li L, Abraham A, Zhou Q, Ali H, O'Brien J, Hamill B *et al*. An improved high yield total synthesis and cytotoxicity study of the marine alkaloid neoamphimedine: an ATP-competitive inhibitor of topoisomerase IIα and potent anticancer agent. *Mar Drugs* 2014; **12**: 4833–4850.

34 Cao H, Xu E, Liu H, Wan L, Lai M. Epithelial-mesenchymal transition in colorectal cancer metastasis: A system review. *Pathol Res Pract* 2015; **211**: 557–569.

35 Kaihara T, Kusaka T, Nishi M, Kawamata H, Imura J, Kitajima K *et al*. Dedifferentiation and decreased expression of adhesion molecules, E-cadherin and ZO-1, in colorectal cancer are closely related to liver metastasis. *J Exp Clin Cancer Res* 2003; **22**: 117–123.

36 Daumar P, Zeglis BM, Ramos N, Divilov V, Sevak KK, Pillarsetty N *et al*. Synthesis and evaluation of (18)F-labeled ATP competitive inhibitors of topoisomerase II as probes for imaging topoisomerase II expression. *Eur J Med Chem* 2014; **86**: 769–781.

37 Furet P, Schoepfer J, Radimerski T, Chene P. Discovery of a new class of catalytic topoisomerase II inhibitors targeting the ATP-binding site by structure based design. Part I. *Bioorg Med Chem Lett* 2009; **19**: 4014–4017.

38 Capdeville R, Buchdunger E, Zimmermann J, Matter A. Glivec (STI571, imatinib), a rationally developed, targeted anticancer drug. *Nat Rev Drug Discov* 2002; **1**: 493–502.

39 Dancey J, Sausville EA. Issues and progress with protein kinase inhibitors for cancer treatment. *Nat Rev Drug Discov* 2003; **2**: 296–313.

40 Jester BW, Cox KJ, Gaj A, Shomin CD, Porter JR, Ghosh I. A coiled-coil enabled split-luciferase three-hybrid system: applied toward profiling inhibitors of protein kinases. *J Am Chem Soc* 2010; **132**: 11727–11735.

41 Korinek V, Barker N, Morin PJ, van Wichen D, de Weger R, Kinzler KW *et al*. Constitutive transcriptional activation by a β-catenin-TCF complex in APC-/- colon carcinoma. *Science* 1997; **275**: 1784–1787.

42 Lovitt CJ, Shelper TB, Avery VM. Advanced cell culture techniques for cancer drug discovery. *Biology (Basel)* 2014; **3**: 345–367.

43 Huang L, Shitashige M, Satow R, Honda K, Ono M, Yun J *et al*. Functional interaction of DNA topoisomerase IIα with the β-catenin and T-cell factor-4 complex. *Gastroenterology* 2007; **133**: 1569–1578.

44 Mosimann C, Hausmann G, Basler K. β-Catenin hits chromatin: regulation of Wnt target gene activation. *Nat Rev Mol Cell Biol* 2009; **10**: 276–286.

45 Nelson JD, Denisenko O, Bomsztyk K. Protocol for the fast chromatin immuno-precipitation (ChIP) method. *Nat Protoc* 2006; **1**: 179–185.

46 Hamada S, Watanabe K, Hirota M, Bianco C, Strizzi L, Mancino M *et al*. Beta-catenin/TCF/LEF regulate expression of the short form human Cripto-1. *Biochem Biophys Res Commun* 2007; **355**: 240–244.

47 Tuli R, Tuli S, Nandi S, Huang X, Manner PA, Hozack WJ *et al*. Transforming growth factor-beta-mediated chondrogenesis of human mesenchymal progenitor cells involves N-cadherin and mitogen-activated protein kinase and Wnt signaling cross-talk. *J Biol Chem* 2003; **278**: 41227–41236.

48 Singh AB, Sharma A, Smith JJ, Krishnan M, Chen X, Eschrich S *et al*. Claudin-1 up-regulates the repressor ZEB-1 to inhibit E-cadherin expression in colon cancer cells. *Gastroenterology* 2011; **141**: 2140–2153.

49 Beck B, Blanpain C. Unravelling cancer stem cell potential. *Nat Rev Cancer* 2013; **13**: 727–738.

50 Fan F, Samuel S, Evans KW, Lu J, Xia L, Zhou Y *et al*. Overexpression of snail induces epithelial-mesenchymal transition and a cancer stem cell-like phenotype in human colorectal cancer cells. *Cancer Med* 2012; **1**: 5–16.

51 Franken NA, Rodermond HM, Stap J, Haveman J, van Bree C. Clonogenic assay of cells in vitro. *Nat Protoc* 2006; **1**: 2315–2319.

52 Wang JC. Interaction between DNA and an *Escherichia coli* protein ω. *J Mol Biol* 1971; **55**: 523–533.

53 Bower JJ, Karaca GF, Zhou Y, Simpson DA, Cordeiro-Stone M, Kaufmann WK. Topoisomerase II α maintains genomic stability through decatenation G(2) checkpoint signaling. *Oncogene* 2010; **29**: 4787–4799.

54 Nitiss JL. DNA topoisomerase II and its growing repertoire of biological functions. *Nat Rev Cancer* 2009; **9**: 327–337.

55 Arce L, Yokoyama NN, Waterman ML. Diversity of LEF/TCF action in development and disease. *Oncogene* 2006; **25**: 7492–7504.

56 Hoverter NP, Zeller MD, McQuade MM, Garibaldi A, Busch A, Selwan EM *et al*. The TCF C-clamp DNA binding domain expands the Wnt transcriptome via alternative target recognition. *Nucleic Acids Res* 2014; **42**: 13615–13632.

57 Bates AD, Berger JM, Maxwell A. The ancestral role of ATP hydrolysis in type II topoisomerases: prevention of DNA double-strand breaks. *Nucleic Acids Res* 2011; **39**: 6327–6339.

58 Szakacs G, Paterson JK, Ludwig JA, Booth-Genthe C, Gottesman MM. Targeting multidrug resistance in cancer. *Nat Rev Drug Disc* 2006; **5**: 219–234.

59 Polakis P. Drugging Wnt signalling in cancer. *EMBO J* 2012; **31**: 2737–2746.

60 Tsavaris N, Lazaris A, Kosmas C, Gouveris P, Kavantzas N, Kopterides P *et al.* Topoisomerase I and IIalpha protein expression in primary colorectal cancer and recurrences following 5-fluorouracil-based adjuvant chemotherapy. *Cancer Chemother Pharmacol* 2009; **64**: 391–398.

61 Gouveris P, Skopelitis E, Tsavaris N. Topoisomerase I and II expression in recurrent colorectal cancer cells: a dubious matter. In: Seligmann H (ed), *DNA Replication-Current Advances.* InTech: Rijeka, Croatia, 2011; pp 639–668.

62 Chavez MS, Scorgie JK, Dennehey BK, Noone S, Tyler JK, Churchill ME. The conformational flexibility of the C-terminus of histone H4 promotes histone octamer and nucleosome stability and yeast viability. *Epigenet Chromatin* 2012; **5**: 5.

Supplementary Information accompanies this paper on the Oncogene website (http://www.nature.com/onc)